

## Analysis Techniques Used On Field Degraded Photovoltaic Modules

By

Thomas D. Hund and David L. King  
Sandia National Laboratories  
PO Box 5800  
Albuquerque, NM 87185-0753

### Introduction

Sandia National Laboratories' PV System Components Department performs comprehensive failure analysis of photovoltaic modules after extended field exposure at various sites around the world. Many of these modules are sent to us because of observed and/or suspected electrical degradation. Sandia maintains a full spectrum of analytical techniques in support of its defense projects, and the photovoltaic program at Sandia uses these resources as needed to help identify the cause of the degradation. This report focuses only on ultrasonic inspection, microscopic inspection, infrared inspection, and module encapsulant adhesion testing. These analytical techniques are used to make solder fatigue life predictions for PV concentrator modules, identify cell damage or current mismatch, and measure the adhesive strength of the module encapsulant. The results help identify the causes of module degradation and provide technical support to the module manufacturers so that they can improve the reliability of their product.

### Ultrasonic Inspection

There are two major methods of ultrasonic inspection: the transmission method and the pulse-echo method. As the names imply, the transmission method measures the ultrasonic energy passing through a test sample, and the pulse-echo method measures the ultrasonic pulse reflected back from defects in the test sample. This technique has been used to identify design and manufacturing problems before module production. After modules are fielded, cell assembly debonding can also be monitored over time using the same techniques (see Figure 1).<sup>1</sup>

The transmission method, which measures only signal attenuation, can only provide information on the size and X-Y location of defects. The sample defects identified by ultrasound are usually voids, cracks, nonuniformities, and debonded laminate structures. The transmission method is limited in sample thickness by the ultrasound attenuation in the material under test; it does not have a minimum sample thickness limitation. Its main advantage is that data interpretation is much less complicated because there are no reflected echoes, just transmitted ultrasound energy.

The pulse-echo method, which is the most frequently used, can locate defects in the Z-axis in addition to measuring the size and the X-Y-axis position. This method measures Z-axis location by measuring the transit time of the reflected pulse. The X-Y location for

This work is supported by the Photovoltaic Energy Technology Division,  
US Department of Energy, contract DE-AC04-94AL85000.

DISTRIBUTION OF THIS DOCUMENT IS UNLIMITED B5

MASTER

RECEIVED  
SEP 26 1995  
OSTI

both methods is established by an X-Y position indicator while the ultrasonic transducer is moved across the sample. Sample thickness is theoretically limited only by the distance the pulse can travel before another pulse is initiated, usually 6 meters. From a practical standpoint, sample thickness is always considerably less than the theoretical limit because of signal attenuation. The minimum sample thickness is limited by the ability of the test equipment to measure the transit time of the echo.

### Ultrasound Test Data

Scan data for the pulse-echo method is presented in three forms, called A-scans, B-scans, and C-scans. The A-scans, which are the most widely used data format, provide a quantitative display of signal amplitudes and time-of-flight data on an oscilloscope screen. The A-scans are used to analyze the type, size, and location of flaws. B-scans display time-of-flight data along a line on the surface of the sample. This data is plotted and used to show size, shape, orientation, and depth of large flaws. C-scans map out signal amplitude and time-of-flight data over the testpiece surface. C-scan data is used to identify defects using a plan view of the testpiece at specific interfaces.

The data in Figure 2 demonstrates the use of the ultrasound technique to detect bond degradation. Nine C-scans and one through-transmission image are displayed from a five-layer stack containing a PV concentrator cell, solder, ceramic insulator, solder, and an aluminum heat spreader. The data shows significant bond degradation at the aluminum/ceramic interface after 250 thermal cycles (-40 to 110°C). As seen in the first row of C-scans, debonding is indicated by the increased pulse-echo signal (dark image) at the aluminum/ceramic interface. The drop in pulse-echo signal at the ceramic/cell interface also indicates debonding at the first interface. It is difficult to make conclusions about the bond at the second interface because most of the pulse-echo is reflected at the debonded first interface. If the first aluminum/ceramic interface were good, then the second interface could be evaluated more effectively for debonding. The third row of pulse-echo scans shows bond degradation throughout the entire cell stack as a function of thermal cycles. The top pulse-echo image is very consistent with the last through-transmission image.

### Metallurgical Cross Section and Scanning Electron Microscopy

A metallurgical cross section and Scanning Electron Microscopy (SEM) were used to measure solder-fatigue crack-growth in a concentrator module cell assembly after 29 months of field use. This destructive analytical technique was necessary because no pre-installation ultrasound scans were available to compare with the field-degraded cell assembly. The only way to measure solder fatigue was with direct microscopic inspection of the fatigue crack (see Figure 3 and 4).<sup>2,3</sup>

Metallurgical cross sections require the cell assembly to be removed from the PV module and cut in half to expose the 0.025-mm (1 mil) thick solder bond between the cell and

## **DISCLAIMER**

**Portions of this document may be illegible  
in electronic image products. Images are  
produced from the best available original  
document.**

copper heat spreader. This is a delicate process and usually requires a special diamond saw to minimize damage to the cell assembly. After all excess material from the cell assembly is removed, the cross section is potted in epoxy for mechanical support and ease of polishing. Polishing dissimilar materials, especially lead solders, requires special polishing compounds and procedures. The 62.5Pb-36.1Sn-1.4Ag eutectic solder alloy has a microstructure that coarsens and elongates when it is exposed to the cyclic strains that cause solder fatigue. Solder fatigue occurs in this cell assembly at the cell-to-copper heat spreader and is caused by daily temperature cycles and the large thermal expansion differences between the silicon (2.6-ppm/°C) and copper heat spreader (16.7 ppm/°C). The effect of solder fatigue is clearly seen in the SEM photos in Figure 5. The Photo #3 microstructure is coarsened and elongated compared with Photo #4. Photo #4 was taken at the center point of the solar cell where cyclic strain was negligible. Photos #1 through #3 were taken from the outer edge of the cell inward to about 1.2 mm.

The SEM images were taken in compositional backscatter mode, which enhances the visibility of the solder microstructure. In this imaging mode a special detector collects electrons that are backscattered from the input electron beam. The number of backscattered electrons increases with higher mass elements, thus making the lead look lighter and the tin look darker.

The percentage area under the cell where the solder had cracked was calculated using the measured crack length on both edges of the solar cell. It was calculated that between 4 and 12% of the area under the cell was debonded due to cracks. This one field degradation measurement was then compared with identical solder fatigue test samples that were cycled under controlled conditions in a temperature cycle chamber. Before and after through-transmission ultrasound scans were used to measure the percent of debonded area in the solder fatigue samples. The fatigue test results are in Figure 6 and show fatigue crack growth for 0 to 80°C, 0 to 100°C, -40 to 110°C, and -50 to 150°C cycles. The one fielded cell assembly solder fatigue measurement after 870 "natural" diurnal cycles resulted in slightly over half the debonded area as the same data point on the 0 to 80°C fatigue curve (see Figure 6).

### **Infrared Imaging**

Infrared imaging of PV modules has proven to be a very useful tool in identifying mismatched cells, cracked cells, and high-resistance contacts caused by failed solder bonds. The infrared camera's spectral bandpass is between 3 and 5 microns and uses a Hg/Cd/Te detector at 77°K. Liquid nitrogen is used to cool the detector and it has a dewar hold time of more than 3 hr. The camera's field of view is 15° vertical and 20° horizontal with a temperature sensitivity of 0.4 to 0.1°C and a spatial resolution of 0.5°/pixel. The entire system consists of a scanner, control electronics, video cassette recorder, and video processing software. Newer infrared cameras do not require the liquid nitrogen, their spatial resolution is closer to 0.1°/pixel, and their image processing is more user friendly.

An infrared scan of a PV module in short-circuit condition is shown in Figure 7. The image indicates that three cells are operating about 5 to 15°C hotter than the rest of the module, and one hot spot is present where a high-resistance solder bond is located. The other cells adjacent to the hot spot are also hotter than normal and they may also have high-resistance contacts or be electrically mismatched with the other cells. In a short-circuit condition, a few cells are typically in reverse bias resulting in internal heating and a temperature higher than the surrounding cells.

### **Encapsulant Adhesion Test**

After 8 to 10 years in the field, loss of adhesion between ethylene vinyl acetate (EVA) and silicon cells has been observed in modules from different manufacturers. In all cases, the modules showing adhesion failure had passed JPL Block V testing at the time of manufacture. This raised concern that the JPL Block V thermal cycle and humidity/freeze tests were unable to identify this particular failure mechanism. In order to answer these questions, a quantitative adhesion test was needed. Sandia has developed a test procedure that will measure EVA adhesive strength to the solar cell.

The test procedure uses either field-degraded modules and/or test modules that have been exposed to environmental testing. First the module is prepared by removing the frame and clamping the glass laminate to a milling machine table. An end-mill is used to remove the Tedlar™ and machine down to the solar cell. A 6-mm diameter cell sample is isolated using a diamond core drill. Care must be taken not to damage the isolated cell fragment or the tempered module glass. Once all EVA residue is removed from the backside of the cell, a stud is epoxied to the cell sample. A load cell mounted in the end-mill is then attached to the stud for the pull test. These procedures quantify the adhesive strength between the top cell surface and the EVA encapsulant (see Figure 8 and 9).

Test results on new modules indicated EVA-to-cell adhesive strengths near  $620 \text{ NT/cm}^2$  ( $900 \text{ lb./in}^2$ ). Work is in progress to measure the effects of environmental aging. In addition to the adhesive strength of the EVA-to-cell interface, the extracted cell sample is available for numerous analytical techniques such as Auger, X-Ray Photoelectron Spectroscopy, and Scanning Electron Microscopy (see Figure 10).

### **Summary**

In summary, the above analytical techniques have helped Sandia identify the cause of different module degradation mechanisms. In all cases, the information obtained was provided to the module manufacturers to assist in improving the reliability of their product.

## DISCLAIMER

### References

This report was prepared as an account of work sponsored by an agency of the United States Government. Neither the United States Government nor any agency thereof, nor any of their employees, makes any warranty, express or implied, or assumes any legal liability or responsibility for the accuracy, completeness, or usefulness of any information, apparatus, product, or process disclosed, or represents that its use would not infringe privately owned rights. Reference herein to any specific commercial product, process, or service by trade name, trademark, manufacturer, or otherwise does not necessarily constitute or imply its endorsement, recommendation, or favoring by the United States Government or any agency thereof. The views and opinions of authors expressed herein do not necessarily state or reflect those of the United States Government or any agency thereof.

- 1) **Nondestructive Evaluation and Quality Control**, Metals Handbook Ninth Edition, Vol. 17, American Society For Metals.
- 2) Joseph I. Goldstein , **Scanning Electron Microscopy and X-Ray Microanalysis**, A Text for Biologists, Materials Scientists, and Geologists, , Plenum Press, 1981.
- 3) D.R. Frear, W.B. Jones, K.R. Kinsman, **Solder Mechanics, A State of the Art Assessment**, Minerals, Metals & Materials Society, 1991.

**Figure 1**

### Ultrasound Of PV Concentrator Cell Assembly

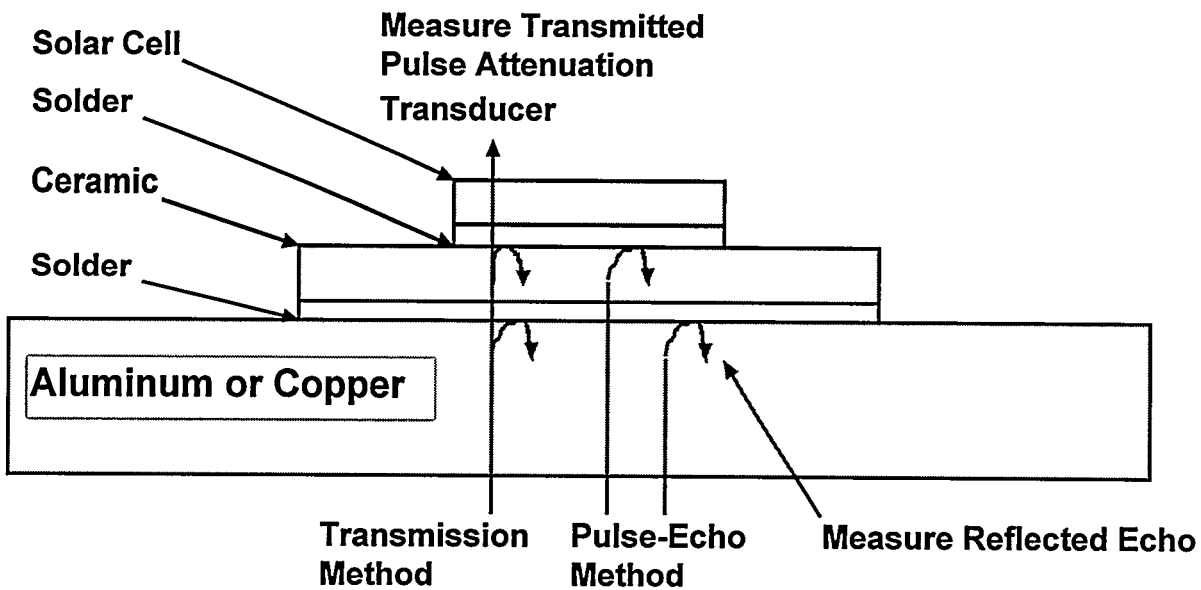


Figure 2

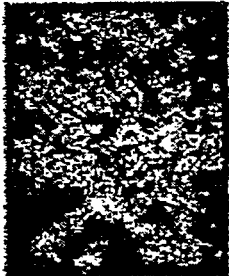
## Nondestructive Ultrasonic Inspection Of PV Concentrator Cell Assemblies

### Pulse-Echo Amplitude At Aluminum/Ceramic Interface

0 Cycles



93 Cycles

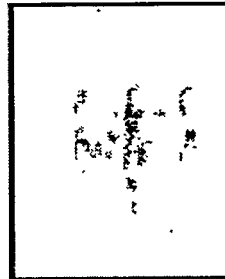
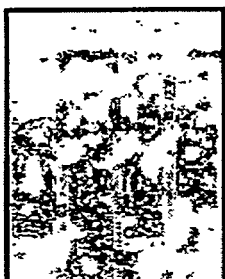


250 Cycles



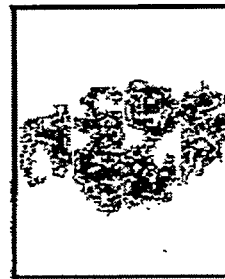
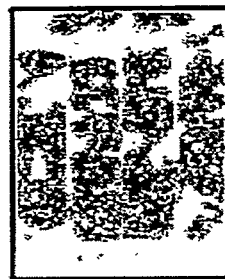
Gray through Black Levels  
Indicate Poor Bond At This  
Interface

### Pulse-Echo Amplitude at Ceramic/Silicon Interface



Gray through Black Levels  
Indicate Good Bonds up to  
this Interface

### Pulse-Echo Amplitude at Top Of Silicon



Gray through Black Levels  
Indicate Good Bonds  
Throughout The Cell

% Debonded

67%

84%

96%

### Through Transmission Image



Gray = No Bond At One Or  
More Interfaces

90%

Figure 3

## PV Concentrator Cell Assembly

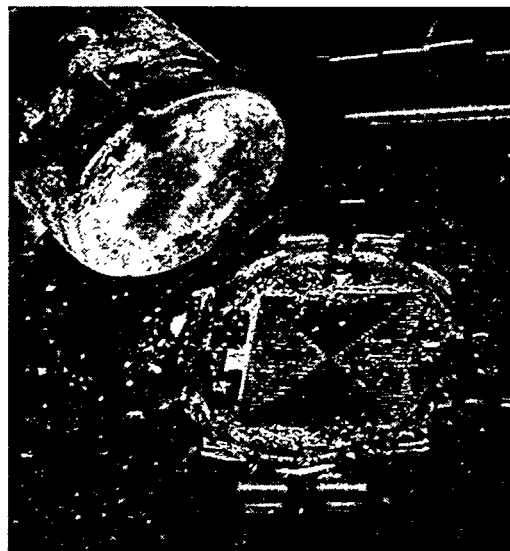


Figure 4

## Solder Fatigue In Cell Assembly After 29 Months

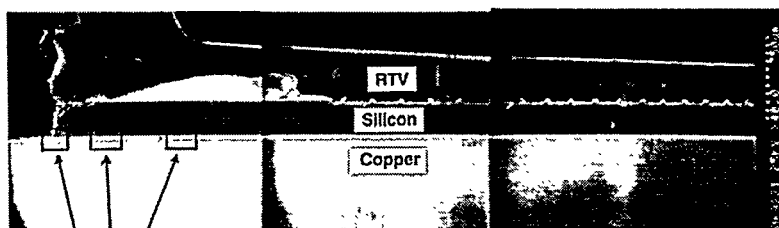


Photo # 1, 2, 3  
Photos of Fatigue Crack Zone  
Crack Length 1.2 mm

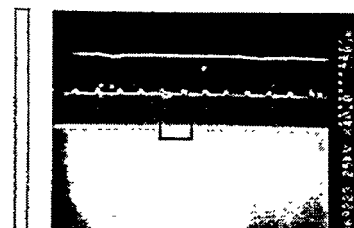
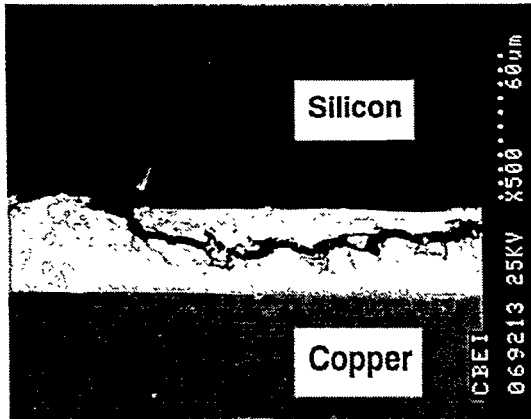


Photo # 4

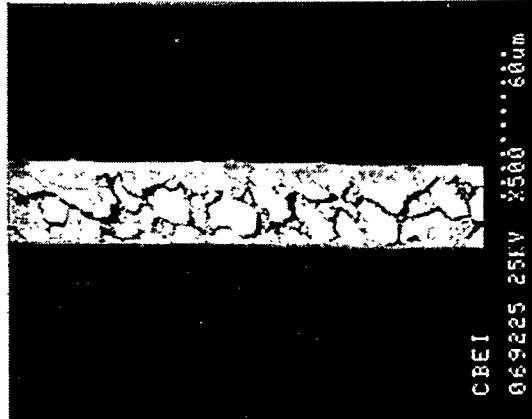


Figure 5

## Solder Fatigue In Cell Assembly After 29 Months



**Photo #1**  
Cell Edge  
Fatigue Crack Initiation



**Photo #2**  
Fatigue Crack Growth

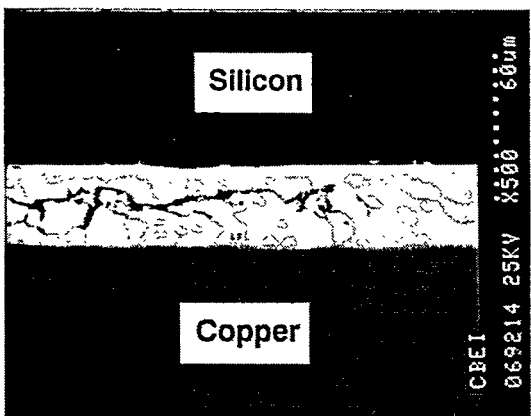


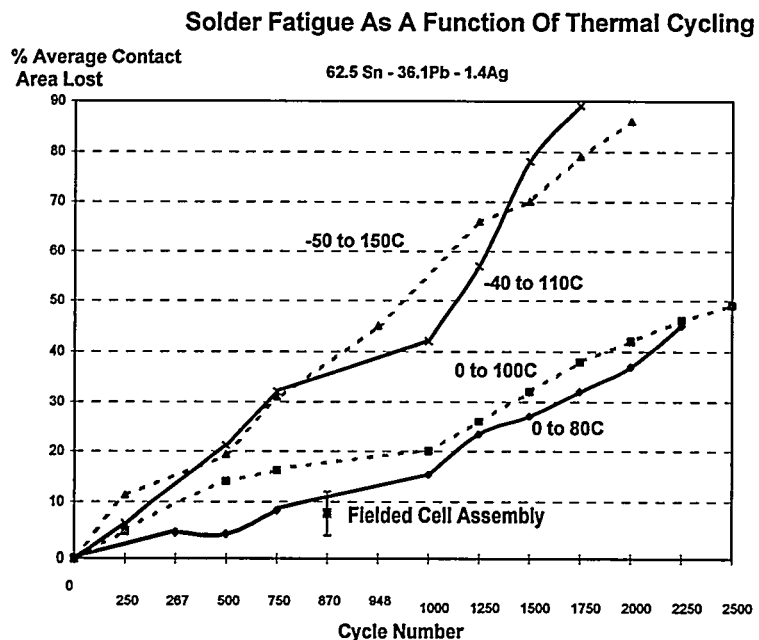
**Photo #3**  
Fatigue Crack Extinction



**Photo #4**  
Cell Center - Undisturbed

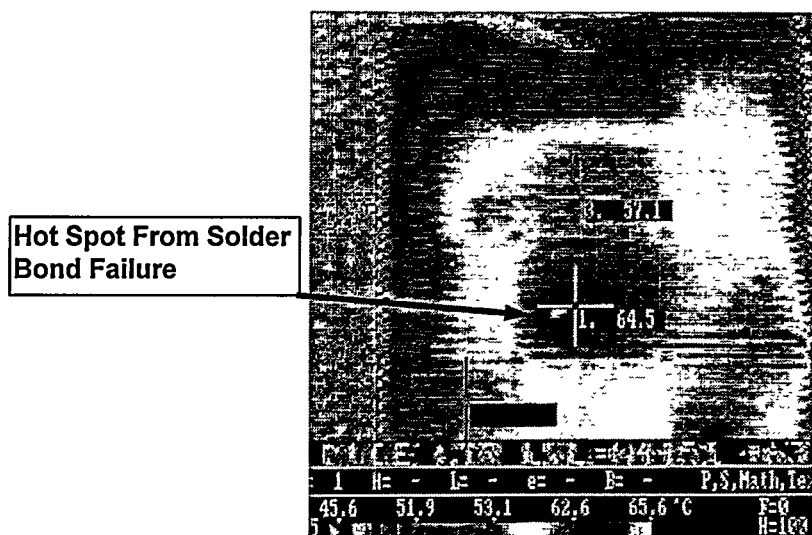


**Figure 6**



**Figure 7**

**Infrared Image Of An Aged  
Crystalline Silicon Module**



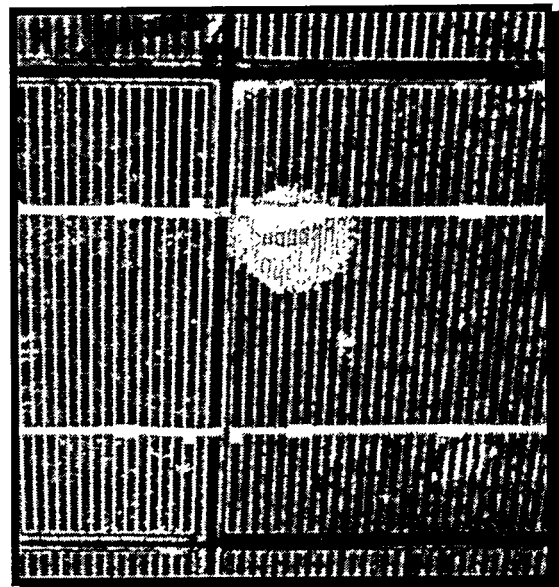
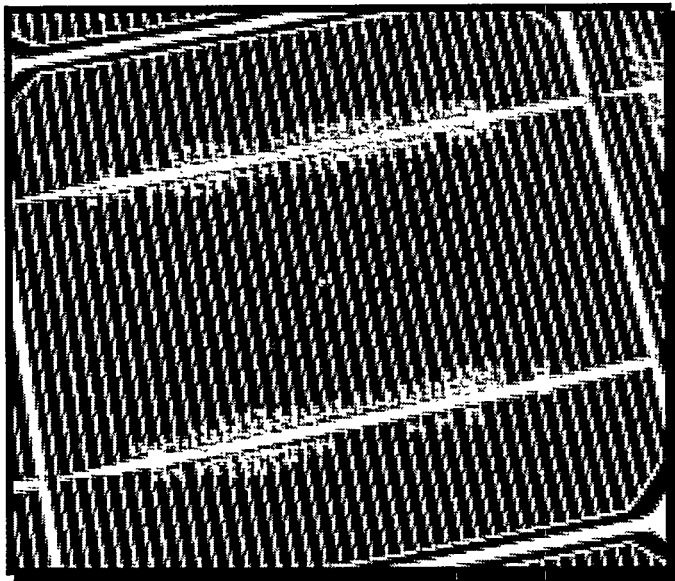
**Sandia  
National  
Laboratories**

Figure 8

## ENCAPSULANT ADHESION

(A Durability Issue)

- ~10-yr. field exposure can result in loss of adhesion at EVA interfaces
- Extent varies, but the problem is common to several manufacturers
- Method developed to quantify adhesion strength at interfaces before and after field exposure or accelerated aging tests



**Sandia  
National  
Laboratories**

Figure 9

## ADHESION STRENGTH TESTING

### Procedure

- Overcome reluctance to hurt a module
- Isolate samples using a milling process
- Bond pull tabs to samples
- Measure tensile stress at failure
- Perform analytical tests (Auger, XPS, SEM, etc.)
- Also solder-bond and EVA samples

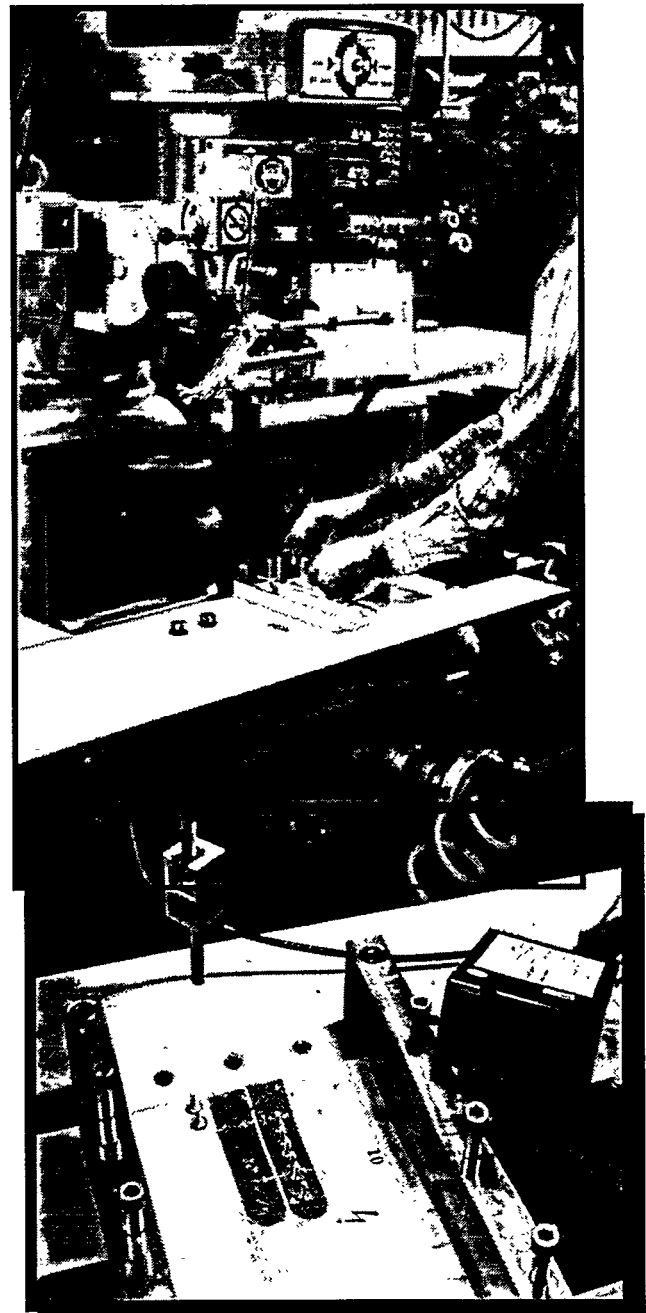
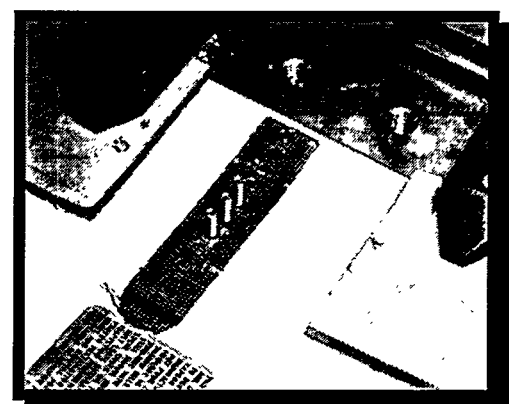
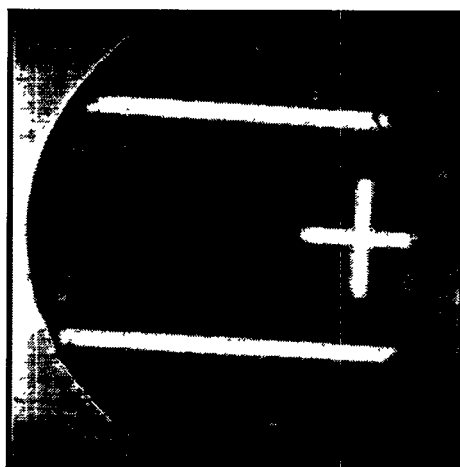


Figure 10

## ADHESION STRENGTH TESTING

### Results

- Repeatable process
- Failure force proportional to sample area
- ~900 lb/in<sup>2</sup> required for failure in new module
- Work in progress to relate failure stress to aging



**Sandia  
National  
Laboratories**